

Water sandwiched by a pair of aromatic rings in a proton-conducting metal-organic framework

Xi-Yan Dong,^{1,2} Xue Li,¹ Bo Li,¹ Yan-Yan Zhu,^{*,1} Shuang-Quan Zang,^{*,1} Ming-Sheng Tang¹

¹ College of Chemistry and Molecular Engineering, Zhengzhou University, Science Road No. 100,
Zhengzhou 450001, China

² College of Chemistry and Chemical Engineering, Henan Polytechnic University, Jiaozuo 454000,
China

Author for correspondence: **Dr. S.-Q. Zang** and **Dr. Y.-Y. Zhu**.

Methods

All reagents and solvents employed in the present work were of analytical grade as obtained from commercial sources without further purification.

Synthesis of $(\text{NH}_4)_2[\text{Ag}_4(\text{mel})(\text{NH}_3)_2]\cdot 3\text{H}_2\text{O}$ (1**):** Excess aqueous NH_3 solution was slowly dropwise added to a suspension of Ag_2O (0.023 g, 0.1 mmol) in $\text{MeOH}/\text{H}_2\text{O}$ (6 mL, 1:1 v/v), and the mixture was stirred for 15 min. H_6mel (0.017 g, 0.05 mmol) was then slowly added to the above mixture, and stirred for 30 min. The resultant colorless solution was allowed to stand in the dark at room temperature for a week to give colorless prism crystals of **1** (yield, 65% based on silver). Anal. Calcd: C, 16.16; H, 2.26; N, 6.28. Found: C, 16.09; H, 2.17; N, 6.13. IR spectrum: 2880-3494(s), 2976(m), 1582(s), 1429(s), 1337(s), 1176(w), 1050(w), 900(s), 842(w), 735(w), 632(m), 502(m).

Physical Measurements. Elemental analyses for C, H, and N were performed on a Perkin-Elmer 240 elemental analyzer. The Fourier transform (FT)-IR spectrum was recorded from KBr pellet in the range from 4000 to 400 cm^{-1} on a Bruker VECTOR 22 spectrometer. Thermal analysis was performed on a SDT 2960 thermal analyzer from room temperature to 500 $^\circ\text{C}$ with a heating rate of 20 $^\circ\text{C}/\text{min}$ under nitrogen flow. Powder X-ray diffraction (PXRD) data for **1** was collected on a Rigaku D/Max-2500PC diffractometer with $\text{Cu-K}\alpha$ radiation ($\lambda = 1.5418 \text{ \AA}$) over the 2θ range of 5–50 $^\circ$ at room temperature.

X-ray Crystallography. Single-crystal data of complex **1** was collected on a Bruker SMART APEX CCD diffractometer with $\text{Mo-K}\alpha$ radiation ($\lambda = 0.71073 \text{ \AA}$) using the

ω scan mode at room temperature. Empirical absorption corrections were applied to the intensities using the SADABS program. The structures were solved using the program SHELXS-97 and refined with the program SHELXL-97. All nonhydrogen atoms were subjected to anisotropic refinement. The hydrogen atoms of the organic ligands were included in the structure factor calculation at idealized positions using a riding model and refined isotropically. The hydrogen atoms of the coordinated and solvent water molecules were located from difference Fourier maps, and then restrained at fixed positions and refined isotropically. The crystallographic data and selected bond distances and angles for **1** are listed in Table 1 and Supporting Information Table S1, respectively. Full details of X-ray crystallographic analysis have been deposited with the Cambridge Crystallographic Data Center under reference number CCDC: 990410 for **1**.

Computation Methods. Models are based on data of **1** from X-ray crystallography. All molecules and complexes were optimized at the M06-2X/6-311++G (d,p) level^{32,33} of theory using Gaussian 09.³⁶ B3LYP-D3 was also used for further confirming the calculation results of M06-2X.^{32,34} The frequency calculations at the same level were carried out to verify the optimized structures to be energy minima with no imaginary frequency. The binding energy of the complexes were calculated using the following formula: "binding energy (BE)" = "energy of the complex" – "energy of the host" – "energy of the guests". And the basis set superposition error (BSSE)¹⁴ of binding energy is calculated using the counterpoise corrections method to obtain more accurate data. Moreover, to estimate the contributions of the lone pairs on

central water oxygen to the $n \rightarrow \pi^*$ interaction ($lp-\pi$, $E_{n \rightarrow \pi^*}$), benzene ring to central water interaction (hydrogen bond, $E_{\pi \rightarrow \sigma^*}$) and intermolecular hydrogen bond among meI^{6-} carboxyl groups and guest molecules, the natural bond orbital (NBO) analysis was carried out at the M06-2X/6-311+G(d,p) level of theory.⁴⁰

AC impedance measurements. Powdered **1** was pressed between copper electrodes in pellet under a pressure of 12–14 M Pa for AC impedance ($Z^* = Z' + iZ''$) measurements. AC impedance spectroscopy measurement was performed on a chi660d (Shanghai Chenhua) electrochemical impedance analyzer with copper electrodes (the purity of Cu is more than 99.8 %) over the frequency range 10^5 –1 Hz. The total pellet resistance (R) is obtained from the intercept of the arc (low-frequency end) on the Z' axis. And the corresponding conductivity (σ) is calculated by the expression $\sigma = d / (RA)$, the thickness (d) and flat surface area (A) of the pellet.

Table S1. Crystallographic data and Structure Refinement for complex **1**.

1	
formula	C ₁₂ H ₂₀ Ag ₄ N ₄ O ₁₅
fw	891.80
cryst syst	monoclinic
space group	<i>P</i> 2 ₁ / <i>c</i>
<i>a</i> (Å)	9.6914(9)
<i>b</i> (Å)	17.9225(16)
<i>c</i> (Å)	13.0999(12)
α (°)	90
β (°)	109.831(10)
γ (°)	90
<i>V</i> (Å ³)	2140.4(3)
<i>Z</i>	4
ρ_{calcd} (g cm ⁻³)	2.767
<i>F</i> (000)	1712
reflns collected	8713
indep reflns	3770
R(int)	0.0319
GOF on <i>F</i> ²	1.005
<i>R</i> ₁ , w <i>R</i> ₂ [<i>I</i> >2σ(<i>I</i>)]	0.0352, 0.0788
<i>R</i> ₁ , w <i>R</i> ₂ (all data)	0.0431, 0.0830

$${}^a R_1 = \frac{\sum ||F_o| - |F_c||}{\sum |F_o|}, {}^b wR_2 = \left\{ \frac{\sum [w(F_o^2 - F_c^2)^2]}{\sum [w(F_o^2)^2]} \right\}^{1/2}$$

Table S2. Selected bond distances and angles for complex **1**.

Bond lengths (Å)			
Ag1–O2	2.261(3)	Ag3–O10#3	2.315(4)
Ag1–O5#1	2.269(3)	Ag3–O7	2.345(3)
Ag1–O4#2	2.455(4)	Ag3–O12#4	2.405(3)
Ag2–N4	2.140(4)	Ag3–Ag4#4	3.1263(7)
Ag2–O8	2.158(3)	Ag4–N3	2.132(4)
Ag2–Ag3	3.0435(7)	Ag4–O11	2.168(3)
Bond Angles (°)			
O2–Ag1–O5#1	123.77(15)	O7–Ag3–Ag2	71.72(8)
O2–Ag1–O4#2	128.25(13)	O12#4–Ag3–Ag2	120.54(8)
O5#1–Ag1–O4#2	103.79(13)	O10#3–Ag3–Ag4#4	72.34(9)
N4–Ag2–O8	170.41(16)	O7–Ag3–Ag4#4	107.94(8)
N4–Ag2–Ag3	99.25(11)	O12#4–Ag3–Ag4#4	66.27(8)
O8–Ag2–Ag3	83.95(9)	Ag2–Ag3–Ag4#4	172.31(2)
O10#3–Ag3–O7	155.75(14)	N3–Ag4–O11	167.58(16)
O10–Ag3–O12#4	122.15(12)	N3–Ag4–Ag3#1	92.81(12)
O7–Ag3–O12#4	77.42(12)	O11–Ag4–Ag3#1	84.98(9)
O10#3–Ag3–Ag2	104.67(9)		

Symmetry codes: #1 $x - 1, y, z$; #2 $-x, -y + 1, -z + 1$; #3 $-x + 1, -y, -z + 1$; #4 $x + 1, y, z$;

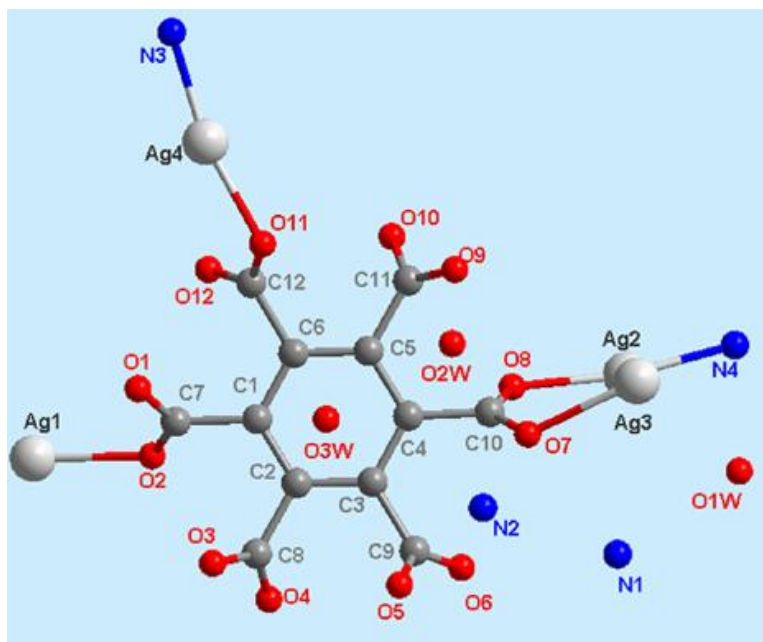


Figure S1. Perspective view of the asymmetric unit. Hydrogen atoms are omitted for clarity.

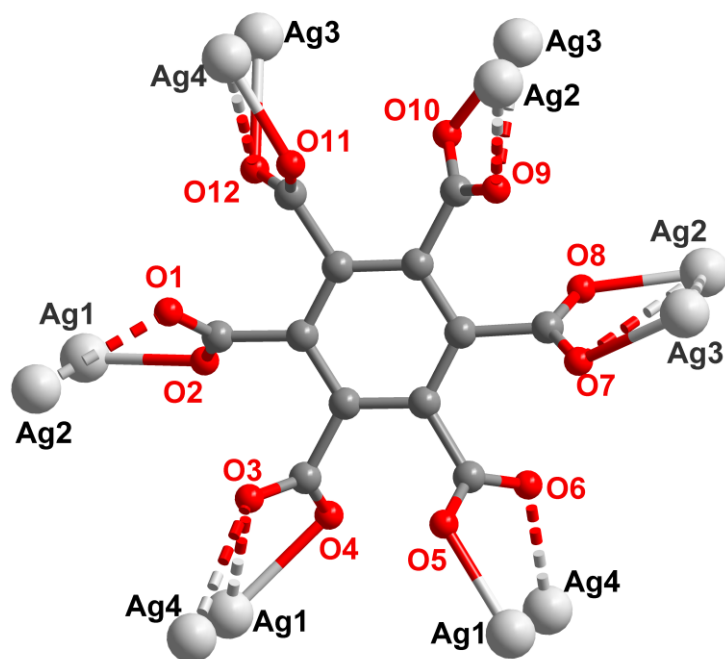


Figure S2. View of the coordination model of mel^{6-} in complex **1**.

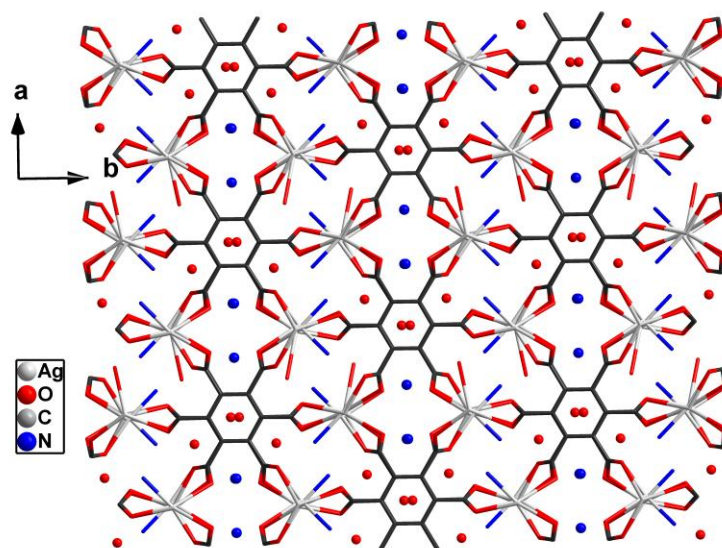


Figure S3. View of three dimensional structure of complex **1** along the *c*-axis. Hydrogen atoms are omitted for clarity.

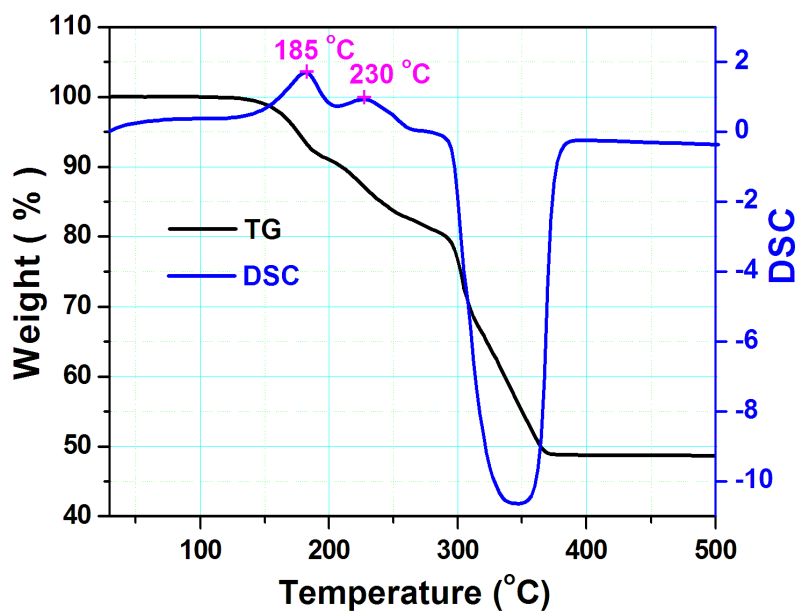


Figure S4. TG plots of as prepared complex **1**.

Table S3. Energy difference of models **Pcw** and **Pcn**, **P1** and **Pn** at the M06-2X/6-311++G(d,p) level using the Gaussian 09 program.

	$ E(\mathbf{Pcw}) - E(\mathbf{Pcn}) $	$ E(\mathbf{P1}) - E(\mathbf{Pn}) $
ΔE (kcal/mol)	22.345	28.697

Table S4. Energy difference of models **Pcw** and **Pcn**, **P1** and **Pn** at the B3LYP-D3/6-311++G(d,p) level using the Gaussian 09 program.

	$ E(\mathbf{Pcw}) - E(\mathbf{Pcn}) $	$ E(\mathbf{P1}) - E(\mathbf{Pn}) $
ΔE (kcal/mol)	24.269	25.353

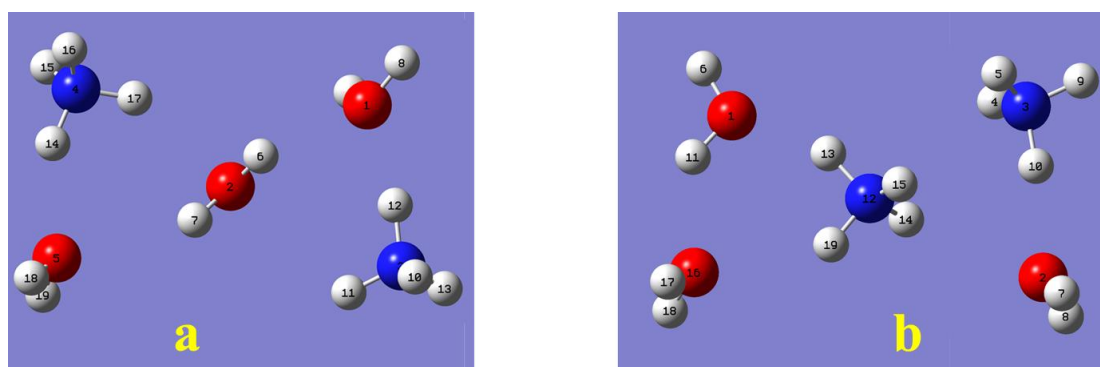


Figure S5. The optimized geometry of **Pcw** (a) and **Pcn** (b) at the M06-2X/6-311++G(d,p) level using the Gaussian 09 program. Model **Pcw** is a pentamer from single-crystal structure of **1**, which includes three water molecules and two ammonium cations with one water molecule located at the center; while Model **Pcn** is another modified pentamer with three water molecules and two ammonium cations, while one ammonium cation at the center.

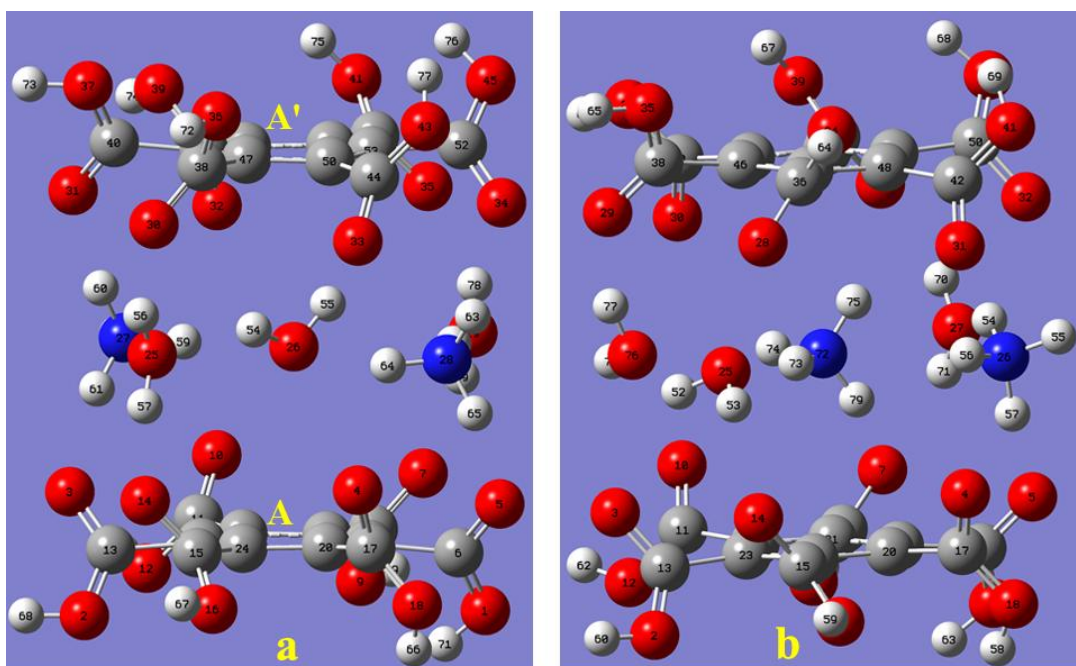


Figure S6. The optimized geometry of **P1** (a) with **Pw** as interlayer and **Pn** (b) with **Pcn** as its interlayer at the M06-2X/6-311++G(d,p) level using the Gaussian 09 program.

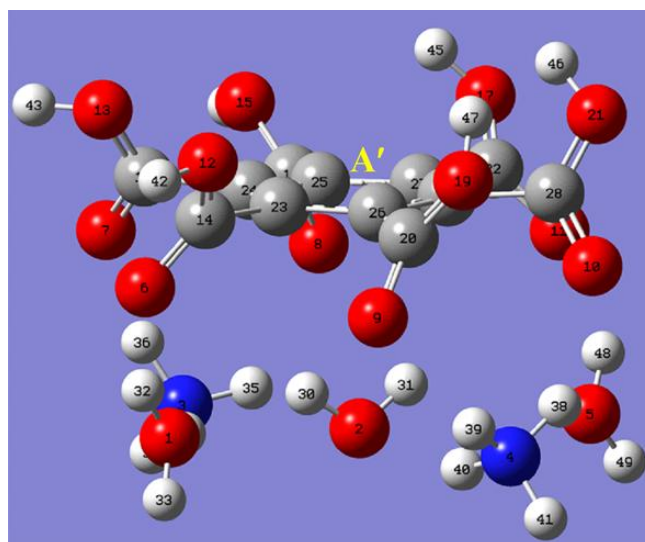


Figure S7. The optimized geometry of **P2** at the M06-2X/6-311++G(d,p) level using the Gaussian 09 program.

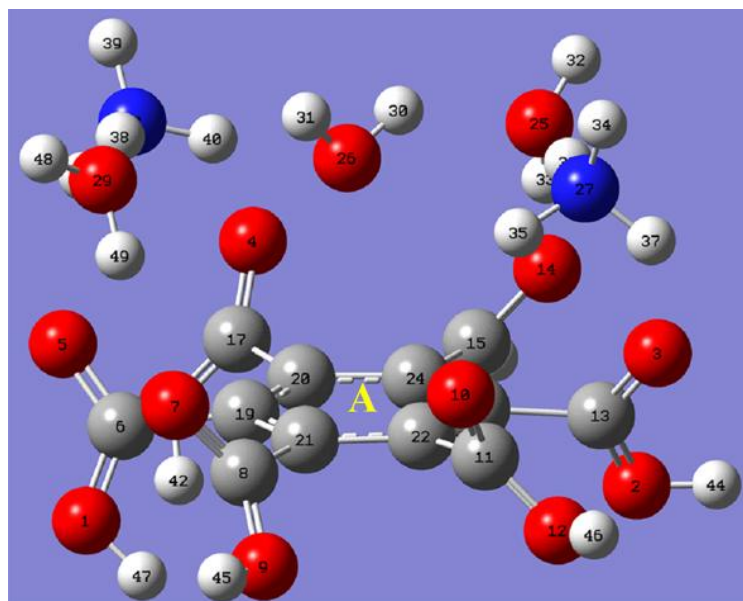


Figure S8. The optimized geometry of **P3** at the M06-2X/6-311++G(d,p) level using the Gaussian 09 program.

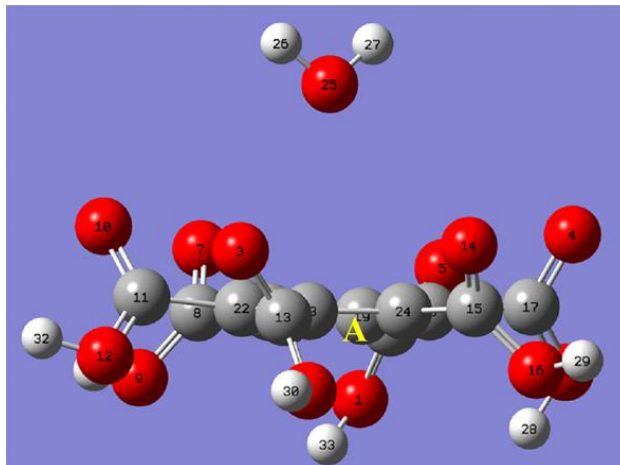


Figure S9. The optimized geometry of **P4** at the M06-2X/6-311++G(d,p) level using the Gaussian 09 program.

Table S5. Binding energies (BE) (in kcal/mol) for models **P1**, **P2**, **P3**, **P4** at the M06-2X/6-311++G(d,p) level using the Gaussian 09 program.

	P1	P2	P3	P4
BE^a	-123.74	-68.53	-73.20	-1.29

^a BE is the binding energy including the basis set superposition error (BSSE) correction.

Table S6. Binding energies (BE) (in kcal/mol) for models **P1**, **P2**, **P3**, **P4** at the B3LYP-D3/6-311++G(d,p) level using the Gaussian 09 program.

	P1	P2	P3	P4
BE^a	-130.75	-71.01	-73.40	-4.70

^a BE is the binding energy including the basis set superposition error (BSSE) correction.

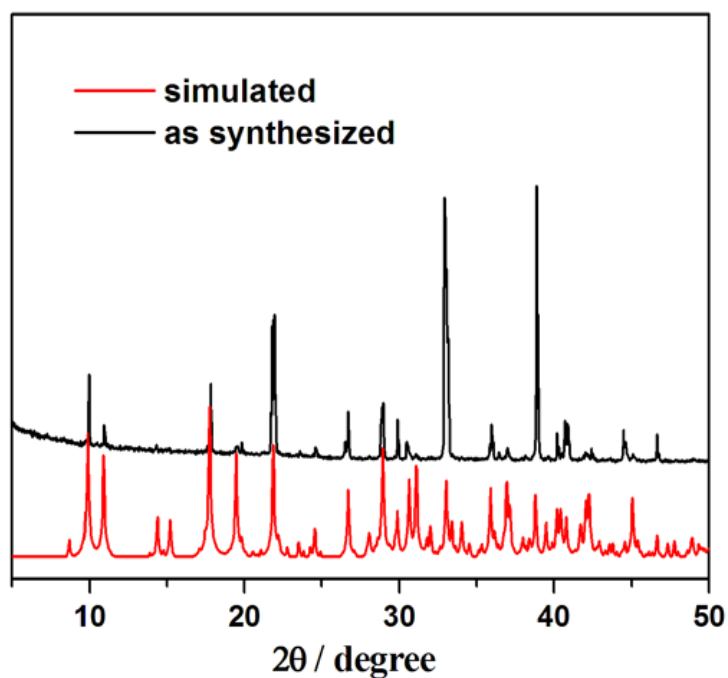


Figure S10. PXRD patterns of **1** and the corresponding simulation according to single crystal structural determinations (red line).

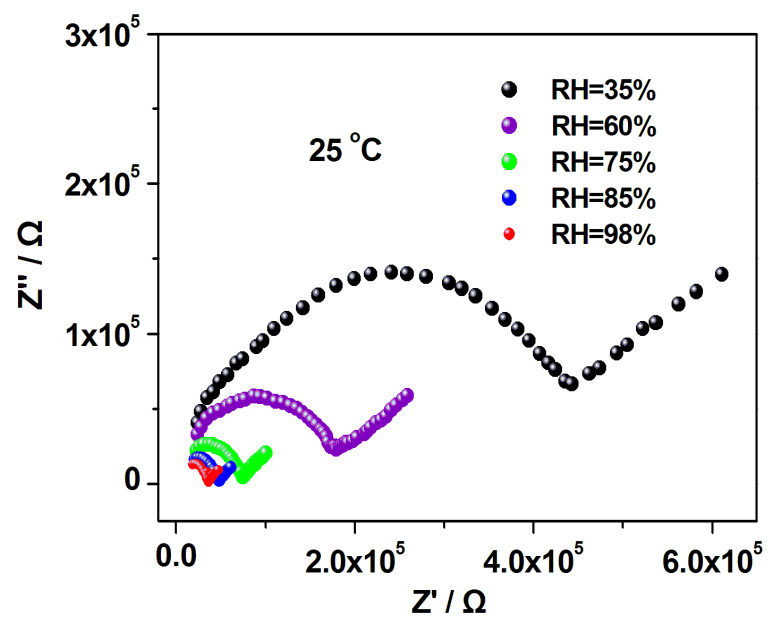


Figure S11. Nyquist plots for **1** at 25°C and different RH.

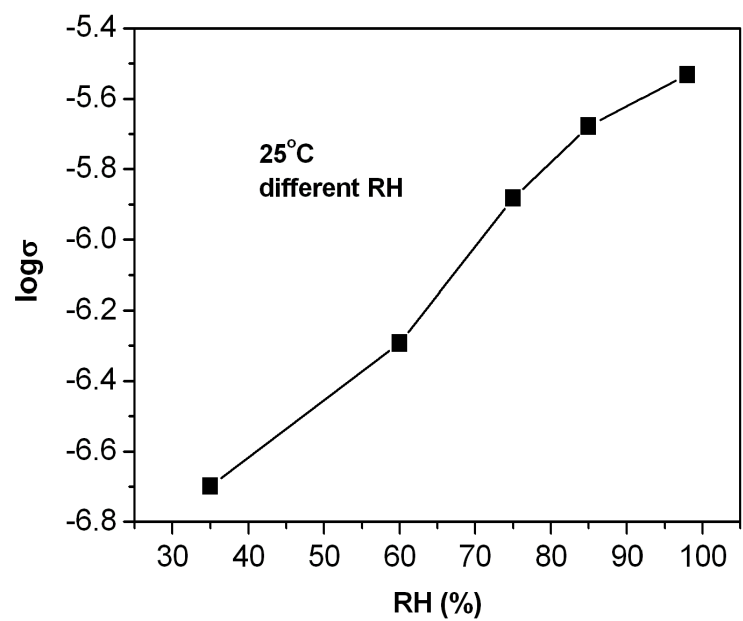


Figure S12. Plot of conductivity (σ) vs relative humidity for **1** at 25°C.

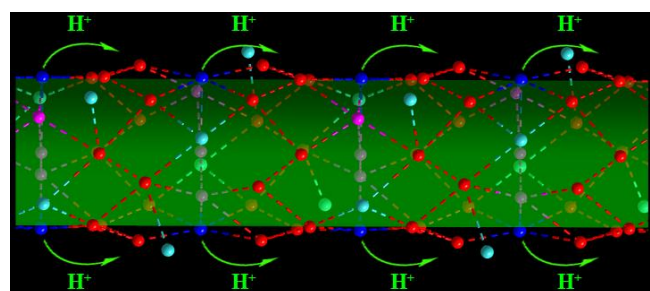


Figure S13. The possible mechanism of proton transport in complex **1**. The colors of blue, turquoise, red, and pink, correspond to ammonium nitrogen, ammonia nitrogen, carboxyl oxygen and water oxygen, respectively.